Received: 7 February 2018 | Revised: 18 April 2018 | Accepted: 24 April 2018
DOI: 10.1002/ardp.201800029

FULL PAPER

DPhG ARCH PHARM
Archiv der Pharmazie

meta-Cyanobenzyl substituted benzimidazolium salts: Synthesis, characterization, crystal structure and carbonic anhydrase, α-glycosidase, butyrylcholinesterase, and acetylcholinesterase inhibitory properties

Ferhat Türker[1] | Duygu Barut Celepci[2] | Aydın Aktaş[1] | Parham Taslimi[3] | Yetkin Gök[1] | Muhittin Aygün[2] | İlhami Gülçin[3]

[1] Faculty of Arts and Sciences, Department of Chemistry, Inönü University, Malatya, Turkey

[2] Faculty of Science, Department of Physics, Dokuz Eylül University, Buca, İzmir, Turkey

[3] Faculty of Science, Department of Chemistry, Ataturk University, Erzurum, Turkey

Correspondence
Dr. Parham Taslimi, Faculty of Science, Department of Chemistry, Ataturk University, 25240-Erzurum, Turkey.
Email: parham_taslimi_un@yahoo.com, parhamsmkh66@gmail.com

Funding information
Dokuz Eylul University, Grant number: 2010.KB.FEN.13

Abstract

meta-Cyanobenzyl-substituted *N*-heterocyclic carbene (NHC) precursors were synthesized by the reaction of a series of *N*-(alkyl)benzimidazolium with 3-bromomethylbenzonitrile. These benzimidazolium salts were characterized by using ^{1}H NMR, ^{13}C NMR, FTIR spectroscopy, and elemental analysis techniques. The molecular and crystal structures of **2f** and **2g** complexes were obtained by using the single-crystal X-ray diffraction method. The derivatives of these novel NHC precursors were effective inhibitors of α-glycosidase (AG), the cytosolic carbonic anhydrase I and II isoforms (hCA I and II), butyrylcholinesterase (BChE), and acetylcholinesterase (AChE) with K_i values in the range of 1.01–2.12 nM for AG, 189.56–402.44 nM for hCA I, 112.50–277.37 nM for hCA II, 95.45–352.58 nM for AChE, and 132.91–571.18 nM for BChE. In the last years, inhibition of the CA enzyme has been considered as a promising factor for pharmacologic intervention in a diversity of disturbances such as obesity, glaucoma, cancer, and epilepsy.

KEYWORDS
α-glycosidase, acetylcholinesterase, butyrylcholinesterase, carbonic anhydrase, enzyme inhibition, *N*-heterocyclic carbene precursors

1 | INTRODUCTION

N-Heterocyclic carbene (NHC) precursors have drawn considerable attention in organometallic chemistry.[1] Especially, numerous studies have been carried out on the catalytic activities of metal-NHC complexes.[2–4] Furthermore, there have been numerous studies on the medical applications of metal-NHCs for the past two decades.[5–8] The chelating effect of NHC precursors with unique sigma donor properties has recently attracted the attention of organometallic chemists. This effect could be effective on biological activity.[9,10] In the studies of biological activity related to NHC precursor and metal-NHC complexes, it is observed that the molecules with bulky and lipophilic properties exhibit higher biological activity.[11,12] In recent years, because of their great structural diversity and multitude of chemical properties, NHCs have been utilized in a variety of capacities. Most recently, NHCs have been utilized as carrier molecules for many transition metals in medicinal chemistry. Specifically, Ag^{+}-NHCs have been investigated as potent antibacterial agents and chemotherapeutics and have shown great efficacy in both *in vitro* and *in vivo* studies.[13,14] Hence we speculated that NHC precursors had the positive charge and linked to the both CA isoenzymes active sides and realized their inhibition effects in these forms.

Carbonic anhydrase isoenzymes (CAs) as zinc metalloenzymes are present in many tissues.[15,16] They catalyze the reversible hydration of water and carbon dioxide to a proton ion and bicarbonate.[17,18] Until now, human cells express 12 catalytically active CA isoenzymes belonging to the class.[19–21] These isoenzymes have been classified into four disparate subclasses based on the subcellular mechanism: secreted (CA VI), cytosolic isoforms (CAs I–III, VII, and XIII), mitochondrial (CAs VA and VB) and membrane-bound (CAs IV, IX, XII, and XIV) forms.[22–26] Additionally, they also have tissue distributions and catalytic activities.[27–29] These isoenzymes play a fundamental role in crucial physiological mechanisms relevant to electrolyte secretion in a variety of tissues/organs, acid-base regulation and respiration, and biosynthetic reactions including ureagenesis, gluconeogenesis, and lipogenesis.[30,31]

The acetylcholinesterase (AChE, E.C.3.1.1.7) enzyme is a particular esterase that belongs to the carboxyl esterase class of enzymes.[32,33] It mostly hydrolyzes the neurotransmitter acetylcholine (ACh). This enzyme is found in high concentrations predominantly in the erythrocyte or red blood cells as well as in the brain cells at cholinergic brain synapses and neuromuscular junctions.[34–37] Additionally, the enzyme butyrylcholinesterase (BChE) which is considered as pseudo cholinesterase (ChE, E.C.3.1.1.8) is a non-specific kind of ChE that hydrolyzes several kinds of ChEs and it ubiquitously exists all over the human body, especially, in the blood serum, human liver, the central neural system, and pancreas.[38,39] In the brain cells, BChE is essentially associated with endothelial cells and glial cells.[40]

Diabetes mellitus (DM) is a chronic disturbance of metabolism caused by a relative or absolute lack of insulin.[41,42] It is determined by hyperglycemia in fasting state and postprandial, and its intense form is associated with protein wasting and ketosis.[43] Enhanced postprandial hyperglycemia (PPHG) is one of the danger agents. PPHG is investigated by the act of α-amylase and α-glycosidase (AG).[44] Inhibition of these metabolic enzymes plays an important role in managing PPHG factors in diabetic patients. Inhibition of AG enzyme gives rise to a diminution in disaccharide hydrolysis, which has useful effects on glycemic index control in diabetic patients.[45]

The studies on the biological activity of NHC compounds containing cyanobenzyl substituents show that these compounds have exhibited biological activity.[11] In this study, we have performed the facile synthesis of well-defined *meta*-cyanobenzyl-substituted NHC precursors (**1** and **2a–g**). The molecular and crystal structure of *meta*-cyanobenzyl **2f** and **2g** were established through single-crystal X-ray diffraction methods. In addition to this study, we have investigated their inhibition potential of hCA I and II isoenzymes, and to discover the most favorable and potent AChE, BChE, and AG inhibition properties of these compounds to give directions to further studies.

2 | RESULTS AND DISCUSSION

2.1 | Chemistry

2.1.1 | Synthesis of the *meta*-cyanobenzyl-substituted benzimidazole and benzimidazolium salts (1, 2a–g)

A series of *meta*-cyanobenzyl-substituted benzimidazole **1** and benzimidazolium salts **2a–g** has been synthesized successfully (Schemes 1 and 2). The effects on enzyme inhibition studies of electronic and steric properties of the *meta*-cyanobenzyl-substituted benzimidazolium salts have been researched. These salts **2a–g** were prepared by mixing 1-aryl-1*H*-benzoimidazole with 1 equivalent of 3-bromomethyl-benzonitrile at 70–110°C for 24 h and were obtained as a white solid in between 81 and 87% yield. All the air and moisture stable benzimidazolium salts were soluble in polar solvents such as water, dimethylsulfoxide, and dimethylformamide. The formation of the new *meta*-cyanobenzyl-substituted benzimidazolium salts was confirmed by FT-IR, ^{1}H NMR and ^{13}C NMR spectroscopic methods, and elemental analysis techniques. These spectra are consistent with the proposed formulate. In the ^{1}H NMR spectra, a characteristic proton peak at the 2-position (NCHN) of the *meta*-cyanobenzyl-substituted benzimidazolium salts **2a–g** was detected, which appeared as highly downfield shifted singlets at δ 10.32, 10.01, 10.13, 10.10, 9.47, 9.42, and 9.34 ppm in the ^{1}H NMR spectra, respectively. The N**C**HN carbon resonances of *meta*-cyanobenzyl-substituted benzimidazolium salts **2a–g** in the ^{13}C NMR spectra appeared highly downfield δ 143.5, 143.7, 143.6, 143.5, 142.3, 142.2, and 142.1 ppm in the ^{13}C NMR spectra. The results of the elemental analysis, in which one of the analytical techniques was used to prove the synthesis of compounds, then the results were evaluated and it was observed that the calculated values were very close to the found values. The FT-IR data clearly indicated the presence of ν(C═N benzimidazole) 1559, 1563, 1557, 1558, 1553, 1563, and 1560 cm^{-1} for the benzimidazolium salts (**2a–g**) proved, respectively. The FT-IR data clearly indicated the presence of ν(C≡N benzonitrile), 2225, 2224, 2227, 2230, 2238, 2228, 2229 cm^{-1} for the benzonitrile group proved, respectively. Also, we obtained single crystal for *meta*-cyanobenzyl-substituted benzimidazolium salts **2f** and **2g** with X-ray diffraction method.

2.2 | Enzyme inhibition results

All the synthesized molecules (novel NHC precursor's derivatives (**1** and **2a–g**)) were tested to investigate their inhibitory activity toward the slower cytosolic isoform (hCA I), the more rapid cytosolic isoenzyme (hCA II), AG, AChE, and BChE enzymes. The chemical formula of *meta*-cyanobenzyl-substituted benzimidazolium salts (**1** and **2a–g**) is given in Scheme 1 and their AChE, BChE, AG, and CA I and II isoforms inhibition data are summarized in Table 1. Novel NHC precursor's derivatives (**1** and **2a–g**) showed effective inhibition

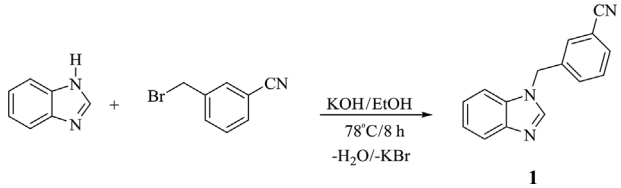

1

SCHEME 1 Synthesis of *meta*-cyanobenzyl-substituted benzimidazolium salts **1**

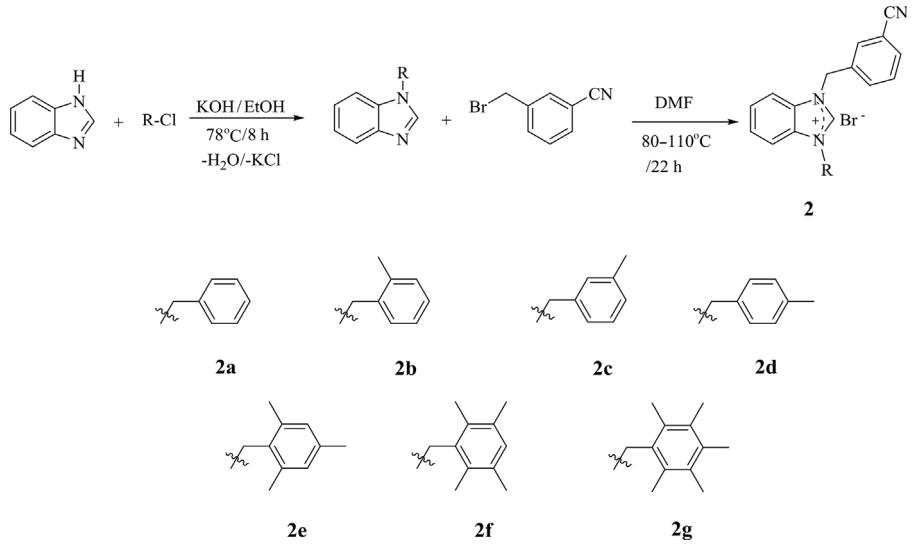

SCHEME 2 Synthesis of *meta*-cyanobenzyl-substituted benzimidazolium salts **2a–g**

profiles against the enzymes mentioned above. The following results are presented in Table 1:

(1) Cytosolic hCA I and II both existed in erythrocyte cells, which are indispensable items for regulating the physiological pH of the blood via manufacturing of HCO_3^-.[46] The cytosolic enzyme hCA I was inhibited by the novel NHC precursor's derivatives (**1**, **2a–g**), with K_i values ranging between 189.56 ± 29.63 and 402.44 ± 97.87 nM. In addition, 1-(3-cyano-benzyl)-3-(2,3,5,6-tetramethyl-benzyl)-3*H*-benzoimidazol-1-ium bromide, **2f** recorded the most powerful hCA I isoform inhibition properties with a K_i value of 189.56 ± 29.63 nM. The clinically and standard used drug acetazolamide (AZA) calculated a K_i value of 501.17 ± 44.17 nM. Thus, the evaluated novel NHC precursor's derivatives (**1** and **2a–g**) showed better inhibitory profiles when compared to AZA molecule (Table 1 and Figure 1).

(2) HCA II has been dependent on various transporters including the Na^+/H^+ exchanger, the Cl^-/HCO_3^- exchanger, and the Na^+/HCO_3^- cotransporter.[47] Indeed, hCA II enzyme is mostly associated with multiple diseases such as glaucoma, renal tubular acidosis, and osteoporosis. It is most largely characterized and studied by the CA isoenzymes.[48] The hCA II was impressively inhibited by the novel NHC precursor's derivatives (**1** and **2a–g**) evaluated here. These molecules shown to strongly inhibit hCA II, with K_i values ranging from 112.50 ± 22.20 to 277.37 ± 64.23 nM. K_i amounts of newly molecules are better than those of the standard used drug AZA (K_i: 382.15 ± 78.11 nM). All the evaluated novel NHC precursor's derivatives (**1** and **2a–g**) showed potent inhibition against hCA II, but the compound of 1-(3-cyano-benzyl)-3-(2,3,4,5,6-pentamethyl-benzyl)-3*H*-benzoimidazol-1-ium bromide, **2g**, showed an significant inhibition profile against hCA II with a K_i value of 112.50 ± 22.20 nM (Table 1, Figures 1 and 2).

(3) AChE and BChE were very strongly inhibited by novel NHC precursor's derivatives (**1** and **2a–g**) (Table 1 and Figure 1). These new molecules had K_i values ranging from 95.45 ± 8.03 to 352.58 ± 43.12 nM for AChE and 132.91 ± 45.53 to 571.18 ± 119.58 nM for BChE. Additionally, tacrine (TAC) compound, used as standard inhibitor, had K_i values of 87.21 ± 14.42 nM toward AChE and 58.36 ± 13.06 nM toward BChE. In this work, all the evaluated novel NHC precursor's derivatives (**1** and **2a–g**) showed potent inhibition against AChE and BChE enzymes, but the compound of 1-(3-cyano-benzyl)-3-(2,4,6-trimethyl-benzyl)-3*H*-benzoimidazol-1-ium bromide, **2e**, for AChE and the compound of 1-(3-cyano-benzyl)-3-(4-methyl-benzyl)-3*H*-benzoimidazol-1-ium bromide, **2d**, for BChE showed excellent inhibition profile against AChE and BChE with K_i values of 95.45 ± 8.03 and 132.91 ± 45.53 nM, respectively (Figure 2).

(4) For the AG enzyme, the novel NHC precursor's derivatives (**1** and **2a–g**) had IC_{50} values in the range of 1.45–2.38 and K_i values in the range of 1.01 ± 0.28–2.12 ± 0.37 nM (Table 1 and Figure 1). The results obviously showed that all novel NHC precursor derivatives (**1** and **2a–g**) demonstrated efficient AG inhibitory effects than that of acarbose (IC_{50}: 22800 nM) as standard AG inhibitor. However, the most effective K_i values were obtained by 1-(3-cyano-benzyl)-3-(4-methyl-benzyl)-3*H*-benzoimidazol-1-ium bromide, **2d**, and 1-(3-cyano-benzyl)-3-(2,3,4,5,6-pentamethyl-benzyl)-3*H*-benzoimidazol-1-ium bromide, **2g**, with K_i values of 1.18 ± 0.51 and 1.01 ± 0.28 nM, respectively.

DM, one of the most prevalent metabolic diseases, is resulting from a shortage in insulin amounts.[49] Type 2 diabetes is considered by hyperglycemia due to defects in insulin action, secretion, or both and has rapidly become a mental and physical burden that diminishes the quality of human life and results in high rates of disability and mortality.[50] Equilibration of postprandial blood glucose amounts is absolutely important, since postprandial hyperglycemia is characterized more hazardous than fasting blood glucose.[51] AG enzyme can release glucose molecule by hydrolyzing branched and linear

TABLE 1 The enzyme inhibition results of novel NHC precursors (**1** and **2a–g**) against human carbonic anhydrase isoenzymes I and II (hCA I and II), acetylcholinesterase (AChE) and butyrylcholinesterase (BChE) and α-glycosidase enzymes

	IC_{50} (nM)									K_i (nM)						
Compounds	hCA I	r^2	hCA II	r^2	AChE	r^2	BChE	r^2	α-Gly	r^2	hCA I	hCA II	AChE	BChE	AChE/BChE	α-Gly
1	302.22	0.9725	234.74	0.9930	337.83	0.9738	452.28	0.9882	2.02	0.9627	279.24 ± 19.33	182.63 ± 33.84	171.47 ± 63.36	353.83 ± 78.03	0.48	1.63 ± 0.66
2a	332.21	0.9854	245.57	0.9854	298.71	0.9861	669.56	0.9789	2.38	0.9763	394.73 ± 52.84	277.37 ± 64.23	128.96 ± 25.38	571.18 ± 119.58	0.22	2.12 ± 0.37
2b	359.62	0.9963	250.18	0.9976	273.37	0.9815	433.12	0.9939	2.13	0.9965	276.63 ± 65.84	224.52 ± 56.92	184.30 ± 2.82	426.56 ± 74.44	0.43	1.37 ± 0.28
2c	346.67	0.9895	171.83	0.9605	375.40	0.9935	538.33	0.9697	1.86	0.9802	320.14 ± 62.66	139.23 ± 32.25	352.58 ± 43.12	245.03 ± 78.06	1.43	1.55 ± 0.21
2d	328.74	0.9994	196.65	0.9662	347.88	0.9943	240.21	0.9825	1.45	0.9681	402.44 ± 97.87	213.32 ± 18.31	166.01 ± 32.94	132.91 ± 45.53	1.25	1.18 ± 0.51
2e	275.43	0.9972	204.12	0.9837	268.18	0.9921	436.94	0.9639	2.37	0.9920	352.36 ± 76.97	194.51 ± 58.54	95.45 ± 8.03	166.94 ± 51.26	0.55	1.85 ± 0.46
2f	318.03	0.9929	260.52	0.9754	319.21	0.9898	382.23	0.9803	1.94	0.9624	189.56 ± 29.63	174.12 ± 41.33	174.70 ± 47.45	306.98 ± 73.30	0.57	1.90 ± 0.70
2g	270.17	0.9909	179.18	0.9572	185.04	0.9865	466.66	0.9683	1.52	0.9831	273.02 ± 69.96	112.50 ± 22.20	159.82 ± 55.46	293.35 ± 66.87	0.54	1.01 ± 0.28
AZA[a]	534.88	0.9680	418.22	0.9778	–	–	–	–	–	–	501.17 ± 44.17	382.15 ± 78.11	–	–	–	–
TAC[b]	–	–	–	–	108.37	0.9709	79.41	0.9688	–	–	–	–	87.21 ± 14.42	58.36 ± 13.06	1.33	–
ACR[c]	–	–	–	–	–	–	–	–	22800	–	–	–	–	–	–	12600 ± 78

[a]Acetazolamide (AZA) was used as a positive control for human carbonic anhydrase I and II isoforms (hCA I and II).
[b]Tacrine (TAC) was used as a positive control for acetylcholinesterase (AChE) and butyrylcholinesterase (BChE) enzymes.
[c]Acarbose (ACR) was used as a positive control for α-glycosidase enzyme. This has been taken from Refs. [94,95].

FIGURE 1 (A) IC_{50} values for hCA I and hCA II isoenzymes, AChE, and BChE enzymes. (B) K_i values for hCA I and hCA II isoenzymes, AChE, and BChE enzymes. (C) IC_{50} and K_i values for α-glycosidase

isomaltose polysaccharides, giving rise to postprandial hyperglycemia. Thus, characterizing and identifying the inhibitors of AG that can be utilized therapeutically is momentous.[52] Commercial AG such as voglibose and acarbose have been used to therapy diabetes, but they exhibit side effects, like acute hepatitis, liver disorders, abdominal

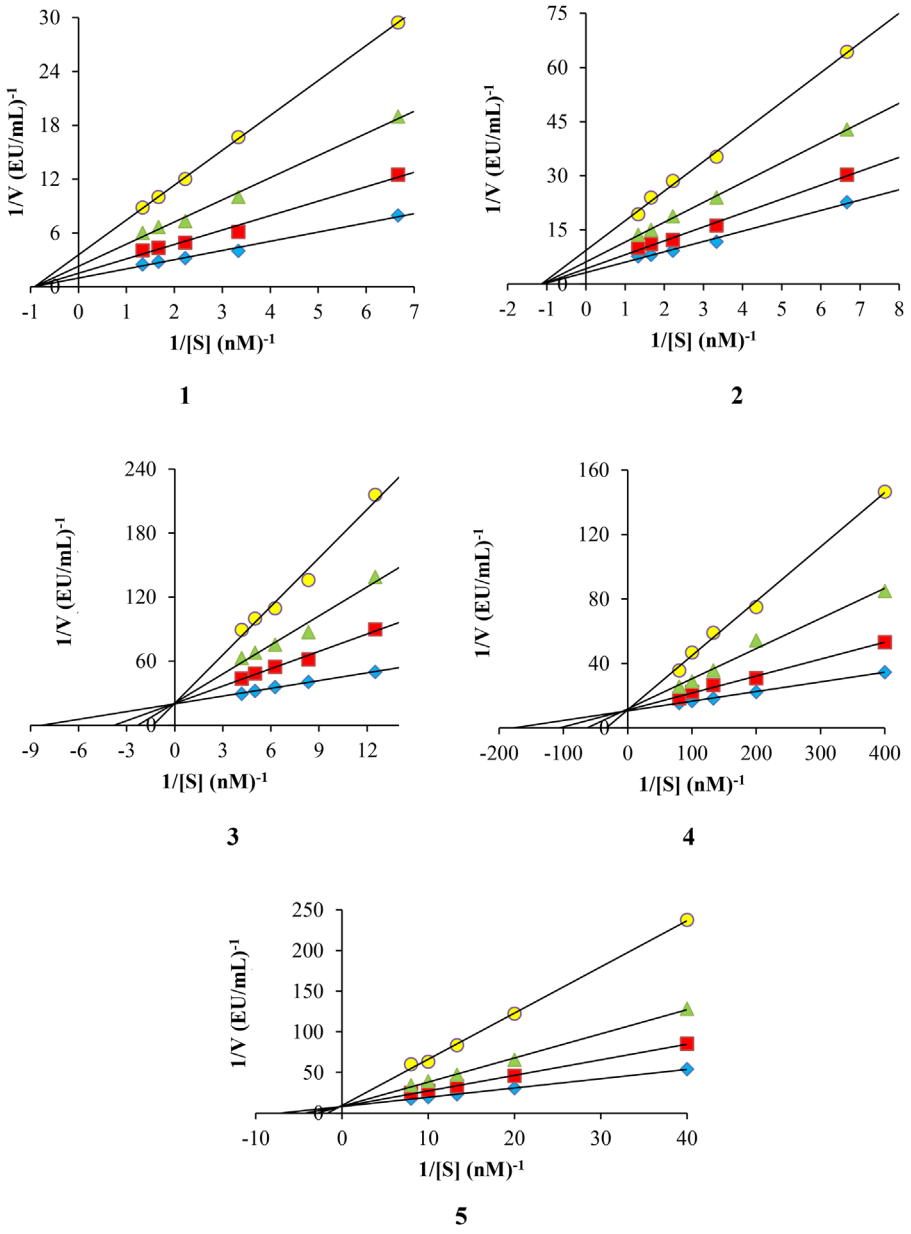

FIGURE 2 K_i graphs of the best inhibitors: (1) hCA I (**2f**), (2) hCA II (**2g**), (3) AChE (**2e**), (4) BChE (**2d**), (5) α-glycosidase (**2g**)

fullness, flatulence, abdominal pain, hepatic injury, renal tumors, and diarrhea.[53]

Recently, a large deal of consideration has been recorded to natural extracts exhibiting AG behaviors, such as those from germ and wheat bran, guava leaves, and grape skins. Several studies have recorded that inflammatory pathways have a significant role linking neurodegenerative diseases such as Alzheimer's disease (AD) and T2DM.[54] However, it has been noted that tissue levels of AChE and BChE and altered plasma can also serve as markers for the entity of slight-grade systemic inflammation in disturbances such as AD and T2DM.[55] Actually, it has been considered that activities of BChE and AChE are elevated in diseases like AD and T2DM including interleukin-6, slight-grade systemic inflammation even when plasma, tissue concentrations and cerebrospinal fluid of C-reactive protein, tumor necrosis factor (TNF-α) and other markers of inflammation are not significantly higher.[56] The acetylcholinesterase inhibitor (AChEI) therapy recorded betterments in the cognitive, functional, and behavioral symptoms related to hypocholinergic states, demonstrated especially by the AD. Many clinical tests using AChEIs for the therapy of AD have been performed. Tacrine compound was the first drug to be trialed and also clinically utilized.[57]

For hCA I isoenzyme (generally considered a significant isoenzyme when CAIs for antiglaucoma or anticancer activity are encountered) was well inhibited by all of the investigated molecules, the best inhibitors of them were 1-(3-cyano-benzyl)-3-(2,3,5,6-tetramethyl-benzyl)-3*H*-benzoimidazol-1-ium bromide, **2f**, 1-(3-cyano-benzyl)-3-(2,3,4,5,6-pentamethyl-benzyl)-3*H*-benzoimidazol-1-ium bromide, **2g** (Figure 1). The 3-benzyl-1-(3-cyano-benzyl)-3*H*-benzoimidazol-1-ium bromide, **2a**, and 1-(3-cyano-benzyl)-3-(4-methyl-benzyl)-3*H*-benzo-imidazol-1-ium bromide, **2d**, compounds are weaker inhibitors

compared to other molecules for this isoenzyme. The compound **2f** was shown to have the excellent inhibitory effect on hCA I isoform activity while the compound **2g** was shown to have the excellent inhibitory effect on hCA I isoform activity. For hCA II isoform, the best inhibitors of them were 1-(3-cyano-benzyl)-3-(3-methyl-benzyl)-3*H*-benzoimidazol-1-ium bromide, **2c**, and 1-(3-cyano-benzyl)-3-(2,3,4,5,6-pentamethyl-benzyl)-3*H*-benzoimidazol-1-ium bromide, **2g**. The 3-benzyl-1-(3-cyano-benzyl)-3*H*-benzoimidazol-1-ium bromide, **2a**, compound is weak inhibitor compared with other compounds for hCA II isoenzyme. As seen in Table 1 and Figure 1, IC_{50} values are in the range of 171.83–250.18 nM toward hCA II, while for hCA I is in the range of 270.17–359.62 nM, and also IC_{50} values for AChE is in the range of 185.04–375.40 nM, while for BChE is in the range of 240.21–669.56. The IC_{50} values for standard molecule AZA toward hCA II and I are 418.22 and 534.88 nM, respectively. All molecules have lower IC_{50} value compared with AZA toward hCA II and hCA I isoenzymes.

CA enzyme reaction is involved in many pathological and physiological processes such as transport of bicarbonate and CO_2 between metabolism lungs and tissues.[58] Examples are electrolyte secretion in various tissues and organs, pH and CO_2 homeostasis, lipogenesis and ureagenesis, glyconeogenesis, calcification, osteoclasis, and tumorigenicity.[59] These mechanisms include CA isoforms that serve as therapeutic aims prone to be inhibited to therapy diverse disturbances such as glaucoma, edema, cancer, obesity, osteoporosis, and epilepsy.[60] CA inhibitors (CAIs) have been utilized clinically as diuretic, antiglaucoma, anti-infective, antiobesity drugs, and anticonvulsant drugs, whereas their functions were only recently recorded in the treatment of hypoxic tumor or cancers. CAIs are a class of chemicals or pharmaceuticals that suppress the CA activity.[61]

2.3 | Crystal structures

The molecular structures of the compounds **2f** and **2g** are shown in Figures 3 and 4. Crystallographic data and refinement details are tabulated in Table 2. The asymmetric units of the compounds are composed of *meta*-cyanobenzyl-substituted benzimidazolium. In **2f**, a tetramethyl-benzyl group is connected to the benzimidazole, whereas in **2g**, a pentamethyl-benzyl group is connected to this moiety. The single crystal X-ray diffraction studies of the compound **2f** indicate that the benzimidazole ring system is substantially planar with the r.m.s deviation of 0.007 Å, and forms dihedral angles of 70.28 (2)° and 101.87 (2)° with the mean plane through the cyanobenzyl and tetramethyl-benzyl rings, respectively. Similarly, the compound **2g** has almost planar benzimidazole ring system with the r.m.s deviation of 0.012. It also forms dihedral angles of 111.76 (1)° and 70.235 (2)° with the mean plane through the cyanobenzyl and pentamethyl-benzyl rings, respectively. The N—C bond lengths for both compounds are complying with the values of similar cyanobenzyl-substituted benzimidazolium salts.[62,63]

In **2f**, two intermolecular hydrogen bonds are observed between the carbon atoms of benzimidazolium and the bromide anion: C1-H1$\cdots$Br1^{i} and C4-H4$\cdots$Br1^{ii}. Molecules propagate one-dimensional infinite chain along the *b*-axis via these hydrogen bonds (Figure 5). The crystal structure of the **2g** is dominated by hydrogen

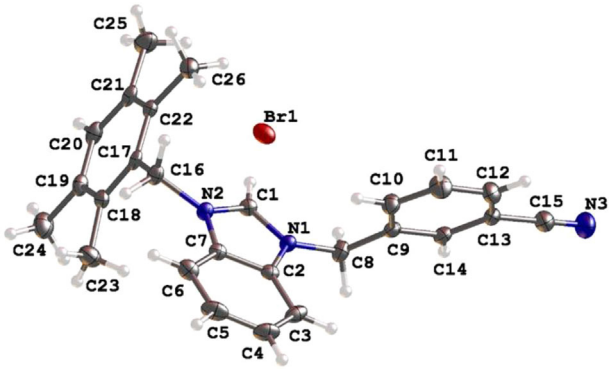

FIGURE 3 The structure of **2f**. Displacement ellipsoids are drawn at the 25% probability level. Selected bond distances (Å) and angles (°): N1-C1 1.3246(1), N1-C2 1.3994(1), N1-C8 1.4575(1), N2-C1 1.3206(1), N2-C7 1.3911(1), N2-C16 1.4720(1), N3-C15 1.1419(1); N1-C1-N2 110.48(3), C1-N1-C8 125.63(3), C1-N2-C16 126.08(3), N1-C8-C9 115.51(3), N2-C16-C17 112.37(3), N3-C15-C11 178.38 (3); N1-C8-C9-C10 1.13(3), C1-N2-C16-C17 39.48(3), N1-C8-C9-C14 −178.61(3)

bonds involving bromide anion and cyano nitrile. Bromide anions act as an acceptor and link the molecules with C8-H8A$\cdots$Br1^{2i} to form a $R_4^2(8)$ graph-set notation. Molecules are also linked by pairs of C10—H10$\cdots$N3^{2ii} hydrogen bonds forming a dimer with the $R_2^2(10)$ graph-set motif. Through these interactions and with the C26—H26B$\cdots$Br1^{2iii} hydrogen bond, the crystal structure forms a three-dimensional network, which is shown in Figure 5.

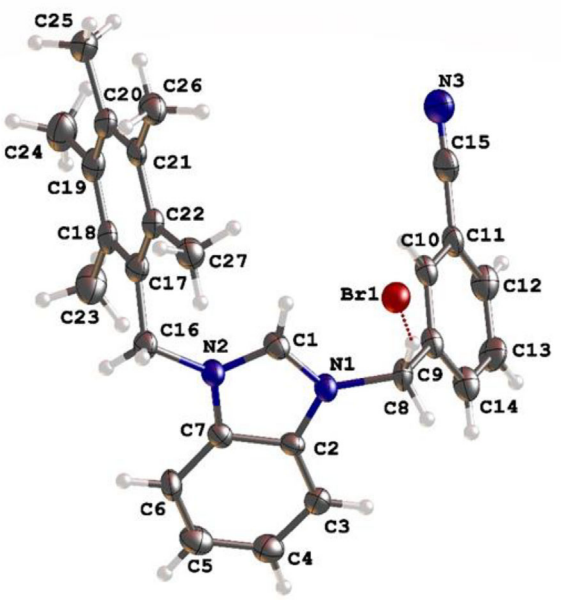

FIGURE 4 The structure of **2g**. Displacement ellipsoids are drawn at the 25% probability level. Selected bond distances (Å), bond angles and torsion angles (°): N1-C1 1.337(2), N1-C2 1.379(2), N1-C8 1.479(2), N2-C1 1.327(2), N2-C7 1.380(2), N2-C16 1.490(2), N3-C15 1.137(2); N1-C1-N2 109.8(7), C1-N1-C8 124.6(7), C1-N2-C16 125.8(7), N1-C8-C9 113.2(7), N2-C16-C17 114.2(7), N3-C15-C11 178.6(2); N1-C8-C9-C10 81.3(9), C1-N2-C16-C17 45.7(2), N1-C8-C9-C14 −99.1(9)

TABLE 2 Crystal data and structural refinement parameters

Compound	2f	2g
Formula	$C_{26}H_{26}BrN_3$	$C_{27}H_{28}BrN_3$
M_r (g/mol)	460.41	474.43
Crystal system	Orthorhombic	Triclinic
Space group	P 21 21 21	P−1
a (Å)	6.3993(4)	8.761(3)
b (Å)	12.5886(10)	10.735(4)
c (Å)	27.767(2)	12.848(5)
α (°)	90	106.19(3)
β (°)	90	90.62(3)
γ (°)	90	94.27(3)
V (Å^3)	2236.8(3)	1156.3(7)
Z	4	2
D_c (g/cm^3)	1.367	1.363
μ (mm^{-1})	1.855	1.797
F (000)	952	492
Crystal size (mm^3)	0.348 × 0.214 × 0.096	0.397 × 0.280 × 0.166
Measured reflections	7245	7144
Independent reflections	3065	4327
GOOF	0.995	1.012
R indices obs. data	R_1 = 0.047 wR_2 = 0.072	R_1 = 0.088 wR_2 = 0.151
R indices all data	R_1 = 0.079 wR_2 = 0.082	R_1 = 0.234 wR_2 = 0.203

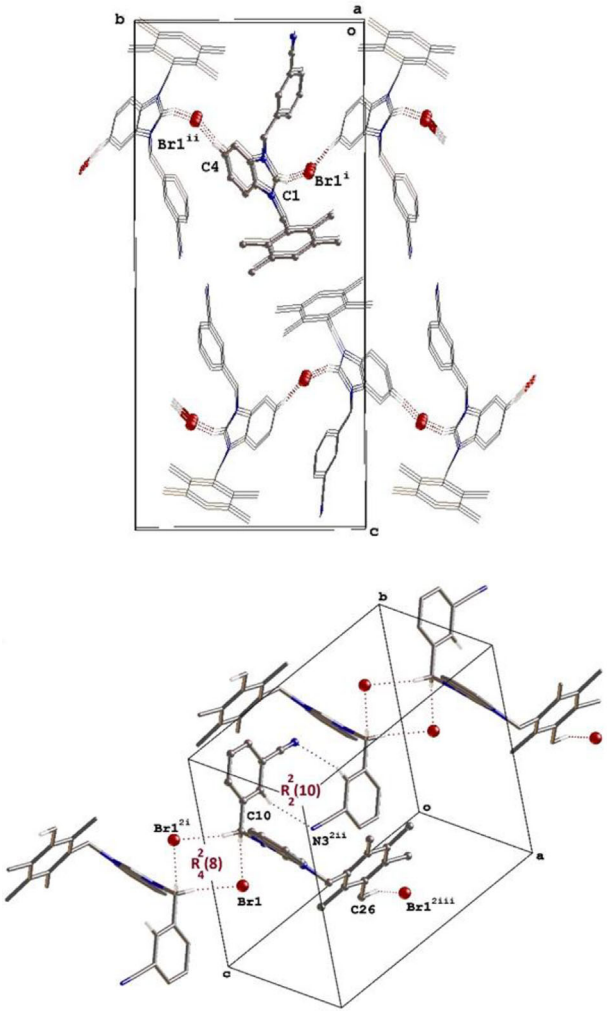

FIGURE 5 (Top) Packing view for the **2f** showing the intermolecular hydrogen bonds C1-H1 ··· Br1^{i} [H1 ··· Br1 2.72 Å, C1-Br1 3.604(3) Å, C1-H1 ··· Br1 158°, symmetry code: (i) 1 + x, y, z], C4-H4 ··· Br1^{ii} [H4 ··· Br1 2.75 Å, C4-Br1 3.631(3) Å, C4-H4 ··· Br1 158°, symmetry code: (ii) −x, 1/2 + y, 1/2 − z]. (Bottom) Packing view for the **2g** showing the intermolecular hydrogen bonds C8-H8A ··· Br1^{2i} [H8A ··· Br1 2.74 Å, C1-Br1 3.698(9) Å, C8-H8A ··· Br1 173°, symmetry code: (2i) −x, 1 − y, 2 − z], C10-H10 ··· N3^{2ii} [H10 ··· N3 2.57 Å, C10-N3 3.443(2) Å, C10-H10 ··· N3 156°, symmetry code: (2ii) −x, 1 − y, 1 − z] and C26-H26B ··· Br1^{2iii} [H26B ··· Br1 2.93 Å, C26-Br1 3.807(2) Å, C26-H26B ··· Br1 153°, symmetry code: (2iii) −x, −y, 1 − z]

3 | CONCLUSIONS

As a result, this study contains the synthesis of the new *meta*-cyanobenzyl-substituted benzimidazolium salts. Also, all of compounds of synthesized have been characterized by using ^{1}H NMR, ^{13}C NMR, FTIR spectroscopy, and elemental analysis techniques. All of the synthesized molecules effectively inhibited some metabolic enzymes such as hCA I, and hCA II, AG, AChE, and BChE enzymes at the nanomolar levels. As we characterized above, novel NHC precursor derivatives (**1** and **2a–g**) can be acceptable candidate drugs, the same as CAIs, for therapy of some diseases such as glaucoma, epilepsy, gastric and duodenal ulcers, osteoporosis, mountain sickness, or neurological disturbances. On the other hand, DM is a metabolic difficulty created by high blood glucose content and can reason other health disturbances, such as neuropathy, weakness, nephropathy retinopathy, high blood pressure, cardiovascular disease, gangrene, and other dysfunctions. Also, these novel compounds can be selective inhibitor AChE, of AG, and BChE enzymes. Structural characterization of the compounds **2f** and **2g** has also been done with single-crystal X-ray diffraction method. Bromide anions have an important role for the stabilization of the crystal structure of both compounds.

4 | EXPERIMENTAL

4.1 | Chemistry

4.1.1 | General

All synthesis containing *meta*-cyanobenzyl-substituted **1a–f** benzimidazolium salts was performed in an inert atmosphere using standard Schlenk techniques. The solvents commercially purchased were used without exposure to any purification and drying process.

All other reagents were commercially available from Merck and Aldrich Chemical Co. and were used without further purification. Melting points were identified in glass capillaries under air with an Electrothermal-9200 melting point apparatus. FT-IR spectra were saved in the range 400–4000 cm^{-1} on Perkin Elmer Spectrum 100 FT-IR spectrometer. Proton (^1H) and carbon (^{13}C) NMR spectra were recorded using either a Bruker 400 Merkur spectrometer operating at 400 MHz (^1H), 100 MHz (^{13}C) in $CDCl_3$ with tetramethylsilane as an internal reference. Elemental analyses were performed by İnönü University Scientific and Technology Centre (İBTAM) (Malatya, Turkey).

The InChI codes of the investigated compounds together with some biological activity data are provided as Supporting Information.

4.1.2 | Synthesis of 3-benzoimidazol-1-ylmethyl-benzonitrile 1

3-Benzoimidazol-1-ylmethyl-benzonitrile **1** was synthesized from the reaction of benzimidazole (3 g, 25 mmol) and 3-bromomethyl-benzonitrile (5 g, 25 mmol) as described in the literature.[64] This known compound was synthesized and characterized by m.p., IR, ^1H and ^{13}C NMR, and microanalyses. Results, which we found, are consistent with the literature.[65] Yield: 5.15 g (87%).

4.1.3 | Synthesis of 3-benzyl-1-(3-cyanobenzyl)-3*H*-benzoimidazol-1-ium bromide 2a

The compound **2a** was synthesized by the reaction of 3-bromomethyl-benzonitrile (1.37 g, 7 mmol) and 1-benzyl-1*H*-benzoimidazole (1.46 g, 7 mmol) in DMF (4 mL). The reaction mixture was stirred for 20 h at 80°C and 2 h at 110°C temperatures. Then the solvents were evaporated under vacuum to afford the product as a white solid. The crude product was recrystallized from ethyl alcohol/diethyl ether (1:3) at room temperature. Yield: 2.32 g (82%); m.p.: 213–214°C; ν(C═N benzimidazole): 1559 cm^{-1}; ν(C≡N benzonitrile): 2225 cm^{-1}. Anal. calcd. for $C_{22}H_{18}BrN_3$: C: 65.36, H: 4.49, N: 10.39. Found: C: 65.41, H: 4.53, N: 10.37. ^1H NMR (400 MHz, DMSO-d_6), δ; 5.85 (s, 2H, —C***H***$_2$(C_6H_4)CN); 5.88 (s, 2H, —C***H***$_2$(C_6H_4)CH_3); 7.42–8.16 (m, 12H, Ar-***H***); 10.32 (s, 1H, 2-C***H***). ^{13}C NMR (100 MHz, DMSO-d_6), δ; 50.3 (—***C***H_2(C_6H_4)CN); 50.5 (—***C***H_2(C_6H_4)CH_3); 114.5, 127.3, 128.1, 128.9, 129.2, 129.5, 131.5, 134.5, and 135.5. (Ar-***C***); 143.5 (2-***C***H).

4.1.4 | Synthesis of 1-(3-cyanobenzyl)-3-(2-methyl-benzyl)-3*H*-benzoimidazol-1-ium bromide 2b

The compound **2b** was synthesized in the same method as that described for **2a**, but 1-(2-methyl-benzyl)-1*H*-benzoimidazole (1.55 g, 7 mmol) was used instead of 1-benzyl-1*H*-benzoimidazole. Yield: 2.49 g (85%); m.p.: 201–202°C; ν(CN benzimidazole): 1563 cm^{-1}; ν(C≡N benzonitrile): 2227 cm^{-1}. Anal. calcd. for $C_{23}H_{20}BrN_3$: C: 66.04, H: 4.82, N: 10.04. Found: C: 66.11, H: 4.86, N: 10.02. ^1H NMR (400 MHz, DMSO-d_6), δ; 2.38 (s, 2H, —CH_2(C_6H_4)C***H***$_3$); 5.85 (s, 2H, —C***H***$_2$(C_6H_4)CN); 5.92 (s, 2H, —C***H***$_2$(C_6H_4)CH_3); 7.25–8.09 (m, 12H, Ar-***H***); 10.01 (s, 1H, 2-C***H***). ^{13}C NMR (100 MHz, DMSO-d_6), δ; 19.4 (—CH_2(C_6H_4)***C***H_3); 49.1 (—***C***H_2(C_6H_4)CN); 49.6 (—***C***H_2(C_6H_4)CH_3); 112.3, 114.5, 114.6, 118.9, 126.9, 127.4, 129.3, 129.1, 129.4, 130.7, 131.3, 132.5, 132.9, and 137.2. (Ar-***C***); 143.7 (2-***C***H).

4.1.5 | Synthesis of 1-(3-cyanobenzyl)-3-(3-methyl-benzyl)-3*H*-benzoimidazol-1-ium bromide 2c

The compound **2c** was synthesized in the same method as that described for **2a**, but 1-(3-methyl-benzyl)-1*H*-benzoimidazole (1.55 g, 7 mmol) was used instead of 1-benzyl-1*H*-benzoimidazole. Yield: 2.42 g (83%); m.p.: 210–211°C; ν(CN benzimidazole): 1557 cm^{-1}; ν(C≡N benzonitrile): 2224 cm^{-1}. Anal. calcd. for $C_{23}H_{20}BrN_3$: C: 66.04, H: 4.82, N: 10.04. Found: C: 66.02, H: 4.84, N: 10.08. ^1H NMR (400 MHz, DMSO-d_6), δ; 2.31 (s, 2H, —CH_2(C_6H_4)C***H***$_3$); 5.77 (s, 2H, —C***H***$_2$(C_6H_4)CN); 5.89 (s, 2H, —C***H***$_2$(C_6H_4)CH_3); 7.20–8.07 (m, 12H, Ar-***H***); 10.13 (s, 1H, 2-C***H***). ^{13}C NMR (100 MHz, DMSO-d_6), δ; 21.4 (—CH_2(C_6H_4)***C***H_3); 49.6 (—***C***H_2(C_6H_4)CN); 50.6 (—***C***H_2(C_6H_4)CH_3); 112.4, 114.4, 114.6, 118.9, 126.0, 127.3, 127.4, 129.3, 129.4, 129.4, 130.7, 132.5, 133.0, and 133.8. (Ar-***C***); 143.6 (2-***C***H).

4.1.6 | Synthesis of 1-(3-cyanobenzyl)-3-(4-methyl-benzyl)-3*H*-benzoimidazol-1-ium bromide 2d

The compound **2d** was synthesized in the same method as that described for **2a**, but 1-(4-methyl-benzyl)-1*H*-benzoimidazole (1.55 g, 7 mmol) was used instead of 1-benzyl-1*H*-benzoimidazole. Yield: 2.52 g (86%); m.p.: 211–212°C; ν(C═N benzimidazole): 1558 cm^{-1}; ν(C≡N benzonitrile): 2230 cm^{-1}. Anal. calcd. for $C_{23}H_{20}BrN_3$: C: 66.04, H: 4.82, N: 10.04. Found: C: 66.08, H: 4.84, N: 10.01. ^1H NMR (400 MHz, DMSO-d_6), δ; 2.30 (s, 2H, —CH_2(C_6H_4)C***H***$_3$); 5.75 (s, 2H, —C***H***$_2$(C_6H_4)CN); 5.88 (s, 2H, —C***H***$_2$(C_6H_4)CH_3); 7.24–8.07 (m, 12H, Ar-***H***); 10.10 (d, 1H, 2-C***H***). ^{13}C NMR (100 MHz, DMSO-d_6), δ; 21.2 (—CH_2(C_6H_4)***C***H_3); 49.6 (—***C***H_2(C_6H_4)CN); 50.5 (—***C***H_2(C_6H_4)CH_3); 112.4, 114.4, 114.6, 118.9, 127.3, 129.0, 130.0, 130.7, 131.6, 132.5, 133.0, 133.8, and 138.7. (Ar-***C***); 143.5 (2-***C***H).

4.1.7 | Synthesis of 1-(3-cyanobenzyl)-3-(2,4,6-trimethyl-benzyl)-3*H*-benzoimidazol-1-ium bromide 2e

The compound **2e** was synthesized in the same method as that described for **2a**, but 1-(2,4,6-trimethyl-benzyl)-1*H*-benzoimidazole (1.75 g, 7 mmol) was used instead of 1-benzyl-1*H*-benzoimidazole. Yield: 2.72 g (87%); m.p.: 268–269°C; ν(CN benzimidazole): 1553 cm^{-1}; ν(C≡N benzonitrile): 2238 cm^{-1}. Anal. calcd. for $C_{25}H_{24}BrN_3$: C: 67.27, H: 5.42, N: 9.41. Found: C: 67.24, H: 5.39, N: 9.44. ^1H NMR (400 MHz, DMSO-d_6), δ; 2.25 and 2.31 (s, 9H, —CH_2(C_6H_2)(C***H***$_3$)$_3$); 5.70 (s, 2H, —C***H***$_2$(C_6H_4)CN); 5.80 (s, 2H, —C***H***$_2$(C_6H_4)CH_3); 7.06 (s, 2H, —CH_2(C_6***H***$_2$)(CH_3)$_3$); 7.61–8.17 (m, 8H, Ar-***H***); 9.47 (s, 1H, 2-C***H***). ^{13}C NMR (100 MHz, DMSO-d_6), δ; 19.9 and 21.2 (—CH_2(C_6H_2)(***C***H_3)$_3$); 45.8 (—***C***H_2(C_6H_4)CH_3); 49.5 (—***C***H_2(C_6H_4)CN); 112.2, 114.4, 114.5, 118.9, 126.2, 127.2, 127.5,

130.0, 130.6, 131.5, 132.1, 132.4, 132.8, 133.3, 136.3, 139.0, and 139.37. (Ar-***C***); 142.3 (2-***C***H).

4.1.8 | Synthesis of 1-(3-cyanobenzyl)-3-(2,3,5,6-tetramethyl-benzyl)-3*H*-benzoimidazol-1-ium bromide 2f

The compound **2f** was synthesized in the same method as that described for **2a**, but 1-(2,3,5,6-tetramethyl-benzyl)-1*H*-benzoimidazole (1.85 g, 7 mmol) was used instead of 1-benzyl-1*H*-benzoimidazole. Yield: 2.61 g (81%); m.p.: 239–240°C; ν(C═N benzimidazole): 1563 cm^{-1}; ν(C≡N benzonitrile): 2228 cm^{-1}. Anal. calcd. for $C_{26}H_{26}BrN_3$: C: 67.83, H: 5.69, N: 9.13. Found: C: 67.78, H: 5.66, N: 9.15. ^{1}H NMR (400 MHz, DMSO-d_6), δ; 2.21 and 2.28 (s, 12H, —$CH_2(C_6H)(CH_3)_4$); 5.77 (s, 2H, —$CH_2(C_6H_4)CN$); 5.82 (s, 2H, —$CH_2(C_6H)(CH_3)_4$); 7.18 (s, 1H, —$CH_2(C_6H)(CH_3)_4$); 7.63–8.25 (m, 8H, Ar-***H***); 9.42 (s, 1H, 2-C***H***). ^{13}C NMR (100 MHz, DMSO-d_6), δ; 15.9 and 20.7 (—$CH_2(C_6H)(CH_3)_4$); 46.5 (—$CH_2(C_6H_4)CN$); 49.5 (—$CH_2(C_6H)(CH_3)_4$); 111.2, 114.4, 114.6, 118.9, 130.6, 132.0, 132.3, 132.8, 133.3, 133.4, 134.7, 135.0, and 136.4. (Ar-***C***); 142.2 (2-***C***H).

4.1.9 | Synthesis of 1-(3-cyanobenzyl)-3-(2,3,4,5,6-pentamethyl-benzyl)-3*H*-benzoimidazol-1-ium bromide 2g

The compound **2g** was synthesized in the same method as that described for **2a**, but 1-(2,3,4,5,6-pentamethyl-benzyl)-1*H*-benzoimidazole (1.95 g, 7 mmol) was used instead of 1-benzyl-1*H*-benzoimidazole. Yield: 2.78 g (84%); m.p.: 228–229°C; ν(C═N benzimidazole): 1560 cm^{-1}; ν(C≡N benzonitrile): 2229 cm^{-1}. Anal. calcd. for $C_{27}H_8BrN_3$: C: 68.35, H: 5.95, N: 8.86. Found: C: 68.37, H: 5.98, N: 8.84. ^{1}H NMR (400 MHz, DMSO-d_6), δ; 2.23 (d, 12H, J = 4 Hz —$CH_2(C_6)(CH_3)_5$); 2.28 (s, 3H, —$CH_2(C_6)(CH_3)_5$); 5.75 (s, 2H, —$CH_2(C_6H_4)CN$); 5.78 (s, 2H, —$CH_2(C_6)(CH_3)_5$); 7.62–8.26 (m, 8H, Ar-***H***); 9.34 (s, 1H, 2-C***H***). ^{13}C NMR (400 MHz, DMSO-d_6), δ; 16.9–17.2 and 17.5 (—$CH_2(C_6)(CH_3)_5$); 47.0 (—$CH_2(C_6H_4)CN$); 49.4 (—$CH_2(C_6)(CH_3)_5$); 112.2, 112.4, 114.3, 114.6, 118.9, 127.3, 130.6, 131.6, 132.0, 132.8, 133.2, 133.5, 134.4, 136.4, and 136.4. (Ar-***C***); 142.1 (2-***C***H).

4.2 | Biochemical studies

4.2.1 | hCA isoenzymes purification and inhibition studies

In this work, both CA isoenzymes were separated and purified by Sepharose-4B-L-tyrosine sulfanilamide affinity chromatography in a single stage.[66–68] The column chemical material of affinity chromatography containing Sepharose-4B-L-tyrosine-sulfanilamide was created conforming to a former procedure.[69,70] The protein molecules flow in the column eluates was spectrophotometrically obtained at 280 nm as explained formerly.[71] CA isoenzymes' activity investigation was obtained using the spectrophotometric style of Verpoorte et al.[72] as described formerly. In this work, changes in absorbance were recorded during 3 min at 348 nm using *p*-nitrophenyl acetate as a substrate which was converted by both isoenzymes to the *p*-nitrophenolate ion compound.[73,74] For estimation of protein quantity, the Bradford[75] way was used during the separation stages. The presence and purity of both isoenzymes were recorded by the SDS–PAGE method.[76]

4.2.2 | AChE/BChE activity determination and inhibition studies

The inhibitory efficacy of novel NHC precursor's derivatives (**1**, **2a–g**) on BChE/AChE activities was obtained conforming to the spectrophotometric procedure of Ellman et al.[77] Butyrylthiocholine iodide (BChI) and also acetylthiocholine iodide (AChI) compounds were used as substrates of the both reactions.[78,79] In this part, 5,5′-dithio-bis(2-nitro-benzoic)acid (DTNB) was used for the estimation of the BChE/AChE activities. Briefly, 100 µL of buffer solution (pH 8.0, Tris/HCl, 1.0 M) and diverse concentration of sample solutions (50–200 µL) dissolved in deionized water were added to 50 µL of BChE/AChE solutions (5.32×10^{-3} EU).[80–82] Then the mixture was incubated for 10 min at 20°C. Finally, 50 µL of DTNB (0.5 mM and 25 mL) of BChI/AChI were added to incubated mixture. Also, the reaction was initiated by the addition of 50 µL of BChI/AChI. Activities of these enzymes were evaluated spectrophotometrically at a wavelength of 412 nm.[83,84]

4.2.3 | Measurement of AG inhibitory activity

AG inhibitory efficacy was performed using *p*-nitrophenyl-D-glycopyranoside (*p*-NPG) as the substrate, according to the procedure of Tao et al.[85] Samples were prepared by dissolving 10 mg in 10 mL ($EtOH/H_2O$). First, 100 µL of phosphate buffer was mixed with 20 µL of the enzyme solution in phosphate buffer (0.15 U/mL, pH 7.4) and 10–100 µL of the sample. Multiple solutions in phosphate buffer were prepared in case of getting full enzyme inhibition. Then it was preincubated at 35°C for 12 min previous by adding the *p*-NPG to the initiation of the reaction.[86] Also, 50 µL of *p*-NPG in phosphate buffer (5 mM, pH 7.4) after preincubation was added and again incubated at 37°C. The absorbances were spectrophotometrically measured at 405 nm.[87] The IC_{50} amount was calculated from activity (%) versus plant concentration plots. Lineweaver–Burk[88] graphs were used to determine V_{max} and other inhibition parameters. The K_i was calculated from these graphs.

4.3 | X-ray crystallography studies

Single crystal X-ray diffraction data were collected at room temperature for **2g** and **2f** on a Rigaku Oxford Xcalibur diffractometer with an Eos-CCD detector using graphite-monochromated Mo-Kα radiation (λ = 0.71073 Å) with CrysAlis^{Pro} software.[89] Data reduction and analytical absorption corrections were performed by CrysAlis^{Pro} program.[90] Utilizing OLEX2,[91] structures were solved by Intrinsic Phasing method with SHELXT[92] and refined by full-matrix least

squares on F^2 in SHELXL.[93] The poor quality of the crystal due to the high mosaicity causes the high *R*-value of **2g**. Anisotropic thermal parameters were applied to all non-hydrogen atoms. All hydrogen atoms were positioned geometrically and refined riding on their respecting carbon atom for both compounds. Bond lengths were fixed at 0.93 Å (aromatic and imidazole carbon H), 0.96 Å (methyl H), and 0.97 Å (methylene H).

ACKNOWLEDGMENT

The authors acknowledge Dokuz Eylul University for the use of the Oxford Rigaku Xcalibur Eos diffractometer (purchased under University Research Grant No: 2010.KB.FEN.13).

CONFLICT OF INTEREST

The authors have declared no conflict of interest.

ORCID

Aydın Aktaş http://orcid.org/0000-0001-8496-6782
Parham Taslimi http://orcid.org/0000-0002-3171-0633

REFERENCES

[1] S. Diez-Gonzalez, N. Marion, S. P. Nolan, *Chem. Rev*. **2009**, *109*, 3612.
[2] Y. Sarı, A. Aktaş, D. B. Celepci, Y. Gök, M. Aygün, *Catal. Lett*. **2017**, *147*, 2340.
[3] A. Aktaş, Y. Gök, *Catal. Lett*. **2015**, *145*, 631.
[4] A. Aktaş, Y. Gök, *Transition Met. Chem*. **2014**, *39*, 925.
[5] I. Yıldırım, A. Aktaş, D. B. Celepci, D. E. Hibbs, Y. Gök, P. A. Williams, B. Hawkins, F. Lai, *Res. Chem. Intermed*. **2017**, *43*, 6379.
[6] S. Akkoç, V. Kayser, I. Ö. İlhan, D. E. Hibbs, Y. Gök, P. A. Williams, B. Hawkins, F. Lai, *J. Organomet. Chem*. **2017**, *839*, 98.
[7] Y. Gök, S. Akkoç, H. Erdoğan, S. Albayrak, *J. Enzyme Inhib. Med. Chem*. **2016**, *31*, 1322.
[8] S. Akkoç, I. Ö. İlhan, Y. Gök, P. J. Upadhyay, V. Kayser, *Inorg. Chim. Acta* **2016**, *449*, 75.
[9] S. Budagumpi, S. Endud, *Organometallics* **2013**, *32*(6), 1537.
[10] Y. Sarı, A. Aktaş, P. Taslimi, Y. Gök, İ. Gülçin, *J. Biochem. Mol. Toxicol*. **2018**, *32*(1), e22009.
[11] A. H. Rosenani, S. Y. Choo, S. Budagumpi, A. A. Abdullah, M. B. K. Ahamed, A. M. S. Abdul Majid, *Inorg. Chim. Acta* **2015**, *433*, 35.
[12] A. Aktaş, Ü. Keleştemur, Y. Gök, S. Balcıoğlu, B. Ateş, M. Aygün, *J. Iran Chem. Soc*. **2018**, *15*, 131.
[13] A. Aktaş, P. Taslimi, İ. Gülçin, Y. Gök, *Arch. Pharm*. **2017**, *350*(6), e1700045.
[14] M. O. Karataş, H. Uslu, S. Sarı, M. A. Alagöz, A. Karakurt, B. Alıcı, C. Bilen, E. Yavuz, N. Gencer, O. Arslan, *J. Enzyme Inhib. Med. Chem*. **2016**, *31*, 760.
[15] P. Taslimi, E. Sujayev, F. Turkan, E. Garibov, Z. Huyut, V. Farzaliyev, S. Mamedova, İ. Gulçin, *J. Biochem. Mol. Toxicol*. **2018**, *32*(2), e22019.
[16] N. Bulut, U. M. Koçyiğit, I. H. Gecibesler, T. Dastan, H. Karci, P. Taslimi, S. Durna Dastan, İ. Gulçin, A. Cetin, *J. Biochem. Mol. Toxicol*. **2018**, *32*(1), e22006.
[17] Y. Akbaba, E. Bastem, F. Topal, İ. Gülçin, A. Maraş, S. Göksu, *Arch. Pharm*. **2014**, *347*, 950.
[18] A. Akıncıoğlu, H. Akıncıoğlu, I. Gülçin, S. Durdağı, C. T. Supuran, S. Göksu, *Bioorg. Med. Chem*. **2015**, *23*, 3592.
[19] B. Arabaci, İ. Gülçin, S. Alwasel, *Molecules* **2014**, *19*, 10103.
[20] Ş. ArasHisar, O. Hisar, Ş. Beydemir, İ. Gülçin, T. Yanık, *Acta Vet. Hung*. **2004**, *52*, 413.
[21] A. Bertucci, A. Moya, S. Tambutté, D. Allemand, C. T. Supuran, D. Zoccola, *Bioorg. Med. Chem*. **2013**, *21*, 1437.
[22] Ş. Beydemir, İ. Gülçin, *J. Enzyme Inhib. Med. Chem*. **2004**, *19*, 193.
[23] T. A. Çoban, Ş. Beydemir, İ. Gülçin, D. Ekinci, *Biol. Pharm. Bull*. **2007**, *30*, 2257.
[24] H. Gocer, F. Topal, M. Topal, M. Küçük, D. Teke, İ. Gülçin, S. H. Alwasel, C. T. Supuran, *J. Enzyme Inhib. Med. Chem*. **2016**, *31*, 441.
[25] U. M. Kocyigit, Y. Budak, M. B. Gürdere, F. Ertürk, B. Yencilek, P. Taslimi, İ. Gulçin, M. Ceylan, *Arch. Physiol. Biochem*. **2018**, *124*(1), 61.
[26] U. M. Koçyiğit, P. Taslimi, H. Gezegen, İ. Gulçin, M. Ceylan, *J. Biochem. Mol. Toxicol*. **2017**, *31*(9), e21938.
[27] H. I. Gul, K. Kucukoglu, C. Yamali, S. Bilginer, H. Yuca, İ. Ozturk, P. Taslimi, İ. Gülçin, C. T. Supuran, *J. Enzyme Inhib. Med. Chem*. **2016**, *31*, 568.
[28] H. I. Gul, E. Mete, P. Taslimi, I. Gulcin, C. T. Supuran, *J. Enzyme Inhib. Med. Chem*. **2017**, *32*, 189.
[29] İ. Gülçin, Ş. Beydemir, M. E. Büyükokuroğlu, *Biol. Pharm. Bull*. **2004**, *27*, 613.
[30] A. Scozzafava, P. Kalın, C. T. Supuran, İ. Gülçin, S. Alwasel, *J. Enzyme Inhib. Med. Chem*. **2015**, *30*, 941.
[31] P. Taslimi, I. Gulcin, B. Ozgeris, S. Goksu, F. Tumer, S. H. Alwasel, C. T. Supuran, *J. Enzyme Inhib. Med. Chem*. **2016**, *31*, 152.
[32] Ç. Bayrak, P. Taslimi, İ. Gülçin, A. Menzek, *Bioorg. Chem*. **2017**, *72*, 359.
[33] İ. Gulçin, M. Abbasova, P. Taslimi, Z. Huyut, L. Safarova, A. Sujayev, V. Farzaliyev, S. Beydemir, S. H. Alwasel, C. T. Supuran, *J. Enzyme Inhib. Med. Chem*. **2017**, *32*, 1174.
[34] U. M. Koçyiğit, A. Taşkıran, P. Taslimi, A. Yokuş, Y. Temel, İ. Gulçin, *J. Biochem. Mol. Toxicol*. **2017**, *31*(11), e21972.
[35] U. M. Kocyigit, Y. Budak, M. B. Gürdere, F. Ertürk, B. Yencilek, P. Taslimi, İ. Gulçin, M. Ceylan, *Synth Commun*. **2017**, *47*(24), 2313.
[36] T. Dastan, U. M. Kocyigit, S. D. Dastan, C. Kiliçkaya, P. Taslimi, Ç. Özge, M. Koparir, A. Çetin, C. Orek, İ. Gulçin, *J. Biochem. Mol. Toxicol*. **2017**, *31*(11), e21971.
[37] P. Taslimi, S. Osmanova, İ. Gulçin, S. Sardarova, V. Farzaliyev, A. Sujayev, R. Kaya, F. Koc, S. Beydemir, S. H. Alwasel, O. I. Kufrevioglu, *J. Biochem. Mol. Toxicol*. **2017**, *31*(9), e21931.
[38] N. Bulut, U. M. Koçyiğit, I. H. Gecibesler, T. Dastan, H. Karci, P. Taslimi, S. Durna Dastan, İ. Gulçin, A. Cetin, *J. Biochem. Mol. Toxicol* **2018**, *32*(1), e22006.
[39] N. Öztaskın, T. Taslimi, A. Maras, S. Göksu, İ. Gülçin, *Bioorg. Chem*. **2017**, *74*, 104.
[40] H. O. Tayeb, H. D. Yang, B. H. Price, F. I. Tarazi, *Pharmacol. Ther*. **2012**, *134*, 8.
[41] L. Zhang, S. Hogan, J. R. Li, S. Sun, C. Canning, S. J. Zheng, K. Zhou, *Food Chem*. **2011**, *126*, 466.
[42] F. Hiroyuki, Y. Tomohide, O. Kazunori, *J. Nutr. Biochem*. **2001**, *12*, 351.
[43] T. Fujisawa, H. Ikegami, K. Inoue, Y. Kawabata, T. Ogihara, *Metabolism* **2005**, *54*, 387.
[44] S. Shobana, Y. N. Sreerama, N. G. Malleshi, *Food Chem*. **2009**, *115*, 1268.
[45] H. Wang, Y. J. Du, H. C. Song, *Food Chem*. **2010**, *123*, 6.
[46] A. Scozzafava, A. Mastrolorenzo, C. T. Supuran, *Expert Opin. Ther. Pat*. **2006**, *16*, 1627.
[47] C. T. Supuran, A. Scozzafava, A. Casini, *Med. Res. Rev*. **2003**, *23*, 146.
[48] C. T. Supuran, A. Casini, A. Mastrolorenzo, A. Scozzafava, *Mini Rev. Med. Chem*. **2004**, *4*, 625.
[49] T. M. C. Adachi, K. Sakurai, N. Shihara, N. Shihara, K. Tsuda, K. Yasuda, *J. Endocrinol*. **2003**, *50*, 271.
[50] H. Laube, *Clin. Drug Investig*. **2002**, *22*, 141.

[51] X. Chen, Y. Zheng, Y. Shen, *Curr. Med. Chem.* **2006**, *13*, 109.
[52] M. Toeller, *Eur. J. Clin. Invest*. **1994**, *24*, 31.
[53] G. Slama, F. Elgrably, A. Sola, J. Mbemba, E. Larger, *Diabetes Metab.* **2006**, *32*, 187.
[54] E. Garibov, P. Taslimi, A. Sujayev, Z. Bingöl, S. Çetinkaya, İ. Gulcin, S. Beydemir, V. Farzaliyev, S. H. Alwasel, C. T. Supuran, *J. Enzyme Inhib. Med. Chem.* **2016**, *31*, 1.
[55] F. Ozbey, P. Taslimi, I. Gulcin, A. Maraş, S. Goksu, C. T. Supuran, *J. Enzyme Inhib. Med. Chem.* **2016**, *31*, 79.
[56] A. Sujayev, E. Garibov, P. Taslimi, İ. Gülçin, S. Gojayeva, V. Farzaliyev, S. H. Alwasel, C. T. Supuran, *J. Enzyme Inhib. Med. Chem.* **2016**, *31*, 1531.
[57] C. Caglayan, I. Gulcin, *J. Biochem. Mol. Toxicol* **2018**, *32*(1), e22010.
[58] H. İ. Gül, M. Tuğrak, H. Sakagami, P. Taslimi, İ. Gülçin, C. T. Supuran, *J. Enzyme Inhib. Med. Chem.* **2016**, *31*, 1619.
[59] A. Innocenti, S. B. Ozturk Sarıkaya, I. Gulcin, C. T. Supuran, *Bioorg. Med. Chem.* **2010**, *18*, 2159.
[60] S. Göksu, A. Naderi, Y. Akbaba, P. Kalın, A. Akıncıoğlu, İ. Gulcin, S. Durdağı, R. E. Salmas, *Bioorg. Chem.* **2014**, *56*, 75.
[61] Y. Sarı, A. Aktaş, P. Taslimi, Y. Gök, İ. Gulçin, *J. Biochem. Mol. Toxicol.* **2018**, *32*(1), e22009.
[62] S. Patil, A. Deally, B. Gleeson, H. Müller-Bunz, F. Paradisi, M. Tacke, *Metallomics* **2011**, *3*, 74.
[63] A. Rosenani, S. Y. Choo, S. Budagumpi, B. Srinivasa, A. Amirul Al-Ashraf, B. Mohamed, A. Khadeer, M. Amin, M. Abdul, *Inorg. Chim.* **2015**, *433*, 35.
[64] B. Christer, E. Aakeröy, J. Desper, J. F. Urbina, *Cryst. Growth Des.* **2005**, *5*, 1283.
[65] A. Rosenani, S. Y. Choo, S. Budagumpi, A. A. Abdullah, M. B. K. Ahmed, A. M. S. A. Majid, *Inorg. Chim. Acta* **2015**, *433*, 35.
[66] Ü. M. Koçyiğit, S. D. Daştan, P. Taslimi, T. Dastan, İ. Gülçin, *J. Biochem. Mol. Toxicol.* **2018**, *32*(1), e22000.
[67] M. Nar, Y. Çetinkaya, İ. Gülçin, A. Menzek, *J. Enzyme Inhib. Med. Chem.* **2013**, *28*, 402.
[68] L. Polat Kose, İ. Gülçin, H. Özdemir, A. Atasever, S. H. Alwasel, C. T. Supuran, *J. Enzyme Inhib. Med. Chem.* **2016**, *31*, 773.
[69] A. Yıldırım, U. Atmaca, A. Keskin, M. Topal, M. Çelik, İ. Gülçin, C. T. Supuran, *Bioorg. Med. Chem.* **2015**, *23*, 2598.
[70] M. Topal, I. Gulcin, *Turk. J. Chem.* **2014**, *38*, 894.
[71] C. Yamali, H. İ. Gul, A. Ece, P. Taslimi, İ. Gülçin, *Chem. Biol. Drug Des.* **2018**, *91*(4), 854.
[72] J. A. Verpoorte, S. Mehta, J. T. Edsall, *J. Biol. Chem.* **1967**, *242*, 4221.
[73] U. M. Kocyigit, Y. Budak, F. Eligüzel, P. Taslimi, D. Kılıç, İ. Gulçin, M. Ceylan, *Arch. Pharm.* **2017**, *350*, e1700198.
[74] C. T. Supuran, *Nat. Rev. Drug Discov.* **2008**, *7*, 168.
[75] M. M. Bradford, *Anal. Biochem.* **1976**, *72*, 248.
[76] P. Taslimi, I. Gulcin, N. Oztaskın, Y. Çetinkaya, S. Göksu, S. H. Alwasel, C. T. Supuran, *J. Enzyme Inhib. Med. Chem.* **2016**, *31*, 603.
[77] G. L. Ellman, K. D. Courtney, V. Andres, R. M. Featherston, *Biochem. Pharmacol.* **1961**, *7*, 88.
[78] M. B. Colovic, D. Z. Krstic, T. D. Lazarevic-Pasti, A. M. Bondžić, V. M. Vasić, *Curr. Neuropharmacol.* **2013**, *11*, 315.
[79] N. Oztaskin, Y. Cetinkaya, P. Taslimi, S. Göksu, İ. Gülçin, *Bioorg. Chem.* **2015**, *60*, 49.
[80] K. Aksu, B. Özgeris, P. Taslimi, A. Naderi, İ. Gülçin, S. Göksu, *Arch. Pharm.* **2016**, *349*, 944.
[81] P. Taslimi, A. Sujayev, E. Garibov, N. Nazarov, Z. Huyut, S. H. Alwasel, İ. Gülçin, *J. Biochem. Mol. Toxicol.* **2017**, *31*(7), e21897.
[82] H. I. Gul, A. Demirtas, G. Ucar, P. Taslimi, İ. Gülçin, *Lett. Drug Des. Discov.* **2017**, *14*, 573.
[83] P. Taslimi, A. Sujayev, S. Mamedova, P. Kalın, İ. Gulcin, N. Sadeghian, S. Beydemir, Ö. İ. Küfrevioglu, S. H. Alwasel, V. Farzaliyev, S. Mamedov, *J. Enzyme Inhib. Med. Chem.* **2017**, *32*, 137.
[84] B. Turan, K. Sendil, E. Sengul, M. S. Gultekin, P. Taslimi, İ. Gulcin, C. T. Supuran, *J. Enzyme Inhib. Med. Chem.* **2016**, *31*, 79.
[85] Y. Tao, Y. Zhang, Y. Cheng, Y. Wang, *Chromatography* **2013**, *27*, 148.
[86] P. Taslimi, C. Caglayan, İ. Gulçin, *J. Biochem. Mol. Toxicol.* **2017**, *31*(12), e21995.
[87] P. Taslimi, H. Akıncıoğlu, İ. Gulçin, *J. Biochem. Mol. Toxicol.* **2017**, *31*(11), e21973.
[88] H. Lineweaver, D. Burk, *J. Am. Chem. Soc.* **1934**, *56*, 658.
[89] CrysAlis^{Pro} Software System, Version 1.171.38.43 (Rigaku Corporation, Oxford, UK, **2015**).
[90] R. C. Clark, J. S. Reid, *Acta Cryst.* **1995**, *51*, 887.
[91] O. V. Dolomanov, L. J. Bourhis, R. J. Gildea, J. A. K. Howard, H. Puschmann, *J. Appl. Cryst.* **2009**, *42*, 339.
[92] G. M. Sheldrick, *Acta Crystallogr.* **2015**, *71*, 3.
[93] S. Parsons, H. D. Flack, T. Wagner, *Acta Cryst.* **2013**, *69*, 249.
[94] M. Torres-Naranjo, A. Suarez, G. Gilardoni, L. Cartuche, P. Flores, V. Morocho, *Molcules* **2016**, *21*, 1461.
[95] H. Teng, L. Chen, T. Fang, B. Yuan, Q. Lin, *J. Funct. Foods* **2017**, *28*, 306.

SUPPORTING INFORMATION

Additional supporting information may be found online in the Supporting Information section at the end of the article.

Crystallographic data as .cif files for the structures reported in this paper have been deposited at the Cambridge Crystallographic Data Center with CCDC 1584233 for compound **2f** and 1584223 for **2g**. Copies of the data can be obtained free of charge at http://www.ccdc.cam.ac.uk/conts/retrieving.html or from the Cambridge Crystallographic Data Center, 12, Union Road, Cambridge CB2 1EZ, UK. Fax: (+44) 1223-336-033, Email: deposit@ccdc.cam.ac.uk.

How to cite this article: Türker F, Barut Celepci D, Aktaş A, et al. *meta*-Cyanobenzyl substituted benzimidazolium salts: Synthesis, characterization, crystal structure and carbonic anhydrase, α-glycosidase, butyrylcholinesterase, and acetylcholinesterase inhibitory properties. *Arch Pharm Chem Life Sci*. 2018;1–11.
https://doi.org/10.1002/ardp.201800029